fermentation

MDPI

Article

Probiotic-Bacteria (*Lactobacillus fermentum*)-Wrapped Zinc Oxide Nanoparticles: Biosynthesis, Characterization, and Antibacterial Activity

Rajeshkumar Shanmugam [1,*], Tharani Munusamy [1], Santhoshkumar Jayakodi [2], Khalid A. Al-Ghanim [3], Marcello Nicoletti [4], Nadezhda Sachivkina [5] and Marimuthu Govindarajan [6,7,*]

1 Department of Pharmacology, Saveetha Dental College and Hospitals, Saveetha Institute of Medical and Technical Science (SIMATS), Chennai 600077, Tamil Nadu, India; tharaninano@gmail.com
2 Department of Biotechnology, Saveetha School of Engineering, Saveetha Institute of Medical and Technical Science (SIMATS), Chennai 602105, Tamil Nadu, India; santhoshkumarj.sse@saveetha.com
3 Department of Zoology, College of Science, King Saud University, Riyadh 11451, Saudi Arabia; kghanim@ksu.edu.sa
4 Department of Environmental Biology, Foundation in Unam Sapientiam, Sapienza University of Rome, 00185 Rome, Italy; marcello.nicoletti@uniroma1.it
5 Department of Microbiology V.S. Kiktenko, Institute of Medicine, Peoples Friendship University of Russia Named after Patrice Lumumba (RUDN University), Moscow 117198, Russia; sachivkina@yandex.ru
6 Unit of Mycology and Parasitology, Department of Zoology, Annamalai University, Annamalainagar 608002, Tamil Nadu, India
7 Unit of Natural Products and Nanotechnology, Department of Zoology, Government College for Women (Autonomous), Kumbakonam 612001, Tamil Nadu, India
* Correspondence: rajeshkumars.sdc@saveetha.com (R.S.); drgovind1979@gmail.com or dr.m.govindarajan@gcwk.ac.in (M.G.)

check for updates

Citation: Shanmugam, R.; Munusamy, T.; Jayakodi, S.; Al-Ghanim, K.A.; Nicoletti, M.; Sachivkina, N.; Govindarajan, M. Probiotic-Bacteria (*Lactobacillus fermentum*)-Wrapped Zinc Oxide Nanoparticles: Biosynthesis, Characterization, and Antibacterial Activity. *Fermentation* **2023**, *9*, 413. https://doi.org/10.3390/fermentation9050413

Academic Editors: Yi-huang Hsueh and Nikos G. Chorianopoulos

Received: 25 March 2023
Revised: 20 April 2023
Accepted: 24 April 2023
Published: 26 April 2023

Abstract: Recently, fabricated nanoparticles (NPs), which can efficiently penetrate biological systems, have found increased usage in the health and hygiene industries. Microbial enzymes and proteins have recently shown their potential to act as reducing agents for the production of NPs, thereby providing an alternative to physical and chemical methods. Not only is this approach efficient and cost-effective, but it also produces a minimal ecological footprint. In this study, zinc oxide nanoparticles (ZnO NPs) were synthesized using probiotic bacteria (*Lactobacillus fermentum*) as the reducing and capping agent. Several analytical methods, including Fourier transform infrared spectroscopy (FT-IR), scanning electron microscopy (SEM), X-ray diffraction analysis (XRD), ultraviolet–visible spectroscopy (UV–Vis), and atomic force microscopy (AFM), were used to analyze the produced ZnO NPs. The SEM analysis confirmed the spherical form of the nanoparticles and estimated their average size to be between 100 and 120 nm. FT-IR analysis verified that the ZnO NPs' surfaces contained many functional groups. X-ray diffraction examination evidenced that the biogenically produced nanoparticles were crystalline. AFM analysis revealed that the nanoparticles' size was about 90–100 nm. The maximum absorption peak, determined via a UV–visible spectrophotometer, was 510 nm. The synthesized ZnO NPs' antimicrobial activity against various bacterial strains was tested, and the highest level of antimicrobial activity was noted against a *Vibrio harveyi* strain. The maximum concentration, namely, 20 mM of ZnO NPs, showed the highest antimicrobial activity. These observations indicate that the synthesized ZnO NPs possess remarkable antimicrobial potency. This method is an efficient, environmentally friendly, cost-effective approach for producing ZnO NPs that are useful for various biomedical applications.

Keywords: green synthesis; nanoparticles; fish pathogen; bio-medicinal application; *Vibrio harvey*; *Lactobacillus fermentum*

1. Introduction

Several essential nutrients, including vitamin D, selenium, iodine, and long-chain Omega-3 fatty acids, can be found in abundant amounts in seafood. Seafood (such as fish) is beneficial to the visual, neuronal, and cognitive development of children and pregnant women [1]; in turn, it can lower the chances of developing cardiovascular disorders [2]. Since the 1950s [3], society has been facing a significant challenge: rising antimicrobial resistance. A number of different antimicrobial agents are currently applied to safeguard marine life against the damage inflicted by pathogenic bacteria. In particular, the extensive use of antimicrobials results in the formation of dangerous byproducts, which have the effect of significantly degrading aquatic habitats, thus having a negative impact on a broad range of animal species and microorganisms [4].

Diseases that may be acquired via seafood are widely acknowledged as being significant public health risks, particularly in industrialized nations. Salmonella and Vibrio are examples of zoonotic bacteria that may cause sickness in humans and aquatic creatures if they are transmitted directly. Ingestion of contaminated seafood or water, both of which often carry zoonotic bacteria, may result in the direct transfer of antibiotic resistance. There is evidence that zoonotic bacteria may contain antimicrobial genes [5]. These pathogens can develop antimicrobial resistance via the inappropriate use of antimicrobial drugs and/or a high frequency of treatment failures. Natural pathogens, such as *Vibrio* spp., *Clostridium botulinum* type F spores, and *Aeromonas*, and enteric bacteria, such as *Campylobacter* and *Salmonella*, are responsible for the contamination of water, especially seawater. In fishery, the commonly found, highly contaminative pathogens include bacteria, mainly from the genera *Salmonella, Noravirus*, *Aeromonas*, and *Vibrio*, which cause great losses and financial damage [6].

Nanoparticles, which may be described as particles having one or more dimensions on the order of 100 nanometers or less, have attracted a lot of attention in recent years. Due to their unusual and interesting features and useful applications, they provide properties that are superior to those of their bulk counterparts. Many different methods from the fields of chemistry, biology, and physics or hybrids thereof may be used to synthesize different nanoparticles. Despite the widespread use of physical and chemical procedures in nanoparticle production, the presence of hazardous chemicals significantly limits their medicinal applications, especially in clinical settings. To further the biological applications of nanoparticles, it is crucial to create processes for their production that are reliable, nontoxic, and ecologically benign. One approach to this objective is the cultivation of microbes for the production of nanoparticles. When compared to nanoparticles produced using chemical processes, those created by means of a biological enzymatic method are far superior. Although chemical techniques can quickly and cheaply produce a wide variety of nanoparticles with precise size and shape specifications, they are also time consuming, labor-intensive, resource-intensive, and wasteful. In fact, they leave behind toxic byproducts that are dangerous to both humans and the environment. The use of costly chemicals is unnecessary or limited in the enzymatic approach. Furthermore, this "green" technique is also beneficial for the environment and society since it uses less energy and confers fewer negative side effects than the chemical alternative [7].

Nanotechnology's potential benefits with respect to agriculture include enhancing product quality, decreasing the risk of pesticide exposure to humans and the environment, increasing crop yields, and securing food supplies in the face of global challenges, such as population growth and climate change. Due to their unique properties, nanoscale materials possess great applicatory potential in the design and development of innovative instruments, which may aid agriculture and other industries. Nanotechnology might improve farming via the utilization of nanoparticle-based fertilizers and through the acceleration of plant growth. Soil quality and agricultural product quality are two areas that may benefit from these enhancements in agriculture. It is also possible, with the help of nanoparticle-based transporters and chemicals, to reduce the number of fertilizers and pesticides used without a corresponding drop in output. Nanotechnology's potential

to minimize waste also lies in its potential to facilitate the production of more efficient products. The utilization of nanosensors in practical settings might pave the way for the more efficient management of agricultural resources, including water, fertilizer, and energy. By using biological processes for the creation of nanomaterials, as is carried out in "green nanotechnology", the possibility for the release of hazardous substances is minimized [8].

One of the most important steps in plant-mediated synthesis is the extraction of bioactive compounds from the plant(s) [9]. However, in modern nanotechnology, the utilization of microorganisms as "nanofactories" offers great potential for synthesizing a broad range of nanoparticles. Fungi and bacteria are now used as feedstock in metal nanoparticle synthesis. By releasing physiologically active molecules such as proteins and enzymes, this process reduces the number of metal ions in nanoparticles. The simple and rapid reproduction of bacteria is becoming increasingly appealing in modern nanotechnology.

The probiotic bacteria of the human superorganism microbiome [10] are predominantly lactic acid Gram-positive microorganisms. They possess thick cell walls composed of polysaccharides, glycosides, proteins, and peptides. These structures are known as bioreduction sites. Due to their negative electric potential, they attract metal ions, ultimately triggering nanoparticle synthesis [11] and protecting against pressure exerted by metal by acting as a protection mechanism [12]. Zinc is a cofactor required for cell growth and nerve impulse transmission [13]. Zinc nanoparticles can be chemically synthesized through methods such as solvent evaporation, the sol–gel method, and microemulsion precipitation techniques. Regarding the development of innovative biomedical materials, the lactic-acid-bacteria-mediated synthesis of nanoparticles can induce different characteristics of zinc oxide nanoparticles (ZnO NPs). However, lactic-acid-bacteria-mediated nanoparticle synthesis is still limited and under development [9].

The production of ZnO nanoparticles by microbes has been documented in a limited number of investigations. However, microbial-mediated nanoparticle synthesis continues to be a promising but underexplored technology. Either an extracellular or an intracellular process might be responsible for the generation of microorganisms. Nanoparticles found outside of cells are known as extracellular nanoparticles. They are made up of biological components, such as glycoproteins, proteins, and metal nanoparticles, that have been attached to the surface of bacteria. Nevertheless, nanoparticles may be synthesized using an intracellular method [14,15], in which particles are first transported into microbial cells and then coupled with catalysts, coenzymes, or proteins. In addition, the use of probiotic strains to manufacture ZnO NPs might be a potential strategy for enhancing the effectiveness of bacteriostatic compounds against medication-blocking and therapeutically relevant infections [16]. In previous research, ZnO NPs were tested against strains of microbial pathogens, including *Aspergillus niger*, *Fusarium oxyspora*, *Penicillium expansum*, *Alternaria alternate*, *Escherichia coli*, *Staphylococcus aureus*, *Pseudomonas aeruginosa*, *Bacillus cereus*, *Klebsiella pneumonia*, *Salmonella typhi*, *Serratia* sp., *Proteus mirabilis*, *Candida albicans*, *Candida tropicalis*, *Streptococcus* sp., and *Bacillus subtilis* [17–21].

Serratia marcescens, which has been listed by the WHO as a dangerous bacterium possessing antibiotic resistance, causes septicemia in fish [22]. *Aeromonas hydrophila* causes *Aeromonas* is, which is a disease characterized by hemorrhagic septicemia, rubella, hemorrhages, abdominal dropsy, abdominal distension, scale loss, edema, and necrosis of the liver and kidneys in fish. As a consequence, infected individuals often suffer from diarrhea. These two pathogens cause Vibriosis in fish, whose clinical picture varies in different fish species, but there are some common signs, including hemorrhages, necrosis, and ulcers on the surface of the body. Vibrions' influence on hemolysin causes anemia in fish. The current study concerns the synthesis of ZnO nanoparticles using the probiotic bacteria *Lactobacillus fermentum* as a reducing and capping gent and subjecting the bacterium to characterization via techniques such as UV–visible spectroscopy, scanning electron microscopy, Fourier transform infrared analysis, and atomic force microscopic analysis. The antibacterial efficacy of the biogenic ZnO nanoparticles was also tested against some fish pathogens, such as *Serratia marcescens, Aeromonas hydrophilla, Vibrio harveyi*, and *Vibrio parahaemolyticus.*

2. Materials and Methods

2.1. Materials

The bacterial cultures *Lactobacillus fermentum* (MTCC 1745), *Serratia marcescens* (MTCC 86), *Aeromonas hydrophilia* (MTCC 1739), *Vibrio harveyi* (MTCC 7030), and *Vibrio parahaemolyticus* (MTCC 451) were collected from MTCC, India. DPPH and other reagents or chemicals were purchased from Sigma Aldrich, India.

2.2. Laboratory Culture of Lactobacillus Fermentum

After obtaining a culture of *L. fermentum*, it was first enriched by inoculating it in Mueller Hinton broth, which was then incubated at 37 °C for twenty-four hours. The broth was then subcultured on a solid medium (Mueller Hinton agar) and placed in an incubator at 37 °C for twenty-four hours. Subculturing was performed at regular intervals in order to preserve the vigor and integrity of the culture, which was grown in Mueller Hinton Agar.

2.3. Synthesis of Nanoparticles

The synthesis of ZnO nanoparticles was accomplished using a bacterial culture consisting of *L. fermentum*. Along with the 1 ml of culture, the precursors zinc acetate and sodium hydroxide were introduced at three different concentrations: 5, 10, and 20 milliMolar. After 10 min of incubation at room temperature to promote aerobic activity, the culture was centrifuged at 10,000 rpm to collect the synthesized nanoparticles. After the pellet had been washed many times with a 0.9% NaCl solution, it was resuspended in a Tris/HCl buffer with a pH of 8.2, and the cells were then subjected to ultrasonication at 100 W for eight minutes. After that, the suspension was centrifuged for 20 minutes at a speed of 10,000 rpm in order to separate the nanoparticles (supernatant) and the deformed cells (pellets). After the ZnO nanoparticles were washed, they were dispersed in double-deionized water after centrifugation at 40,000 rpm for 30 min.

2.4. Characterization of Nanoparticles

Various techniques were utilized for nanoparticle characterization [23], including X-Ray diffraction (Perkin Emler spectrum one instrument, Waltham, MA, USA), the Fourier transform infrared technique (using a Shimadzu spectroscopy Model IRAffinity-1, with a wave number range of about 4000–400 cm^{-1} and a resolution of about 4–8 cm, Kyoto, Japan), scanning electron microscopy (ZEISS (EVO18) Japan; Model—Nanosurf easy scan 2 AFM, Hombrechtikon, Switzerland), and UV–vis spectroscopy (UV-2450, Shimadzu). The optical characteristics of samples were determined using a UV–Visible spectrophotometer, which was operated in the range of 300–800 nm.

2.5. Antibacterial Activity Evaluation

The protocol of Ref. [18] was followed with minimal modifications. The antibacterial activity was determined by adopting the agar well diffusion technique. The antimicrobial activity of the synthesized NPs against strains of *Serratia marcescens*, *Aeromonas hydrophilia*, *Vibrio harveyi*, and *Vibrio parahaemolyticus* was tested. Mueller Hinton Agar-Hi Media (250 mL) was prepared and poured into sterilized Petri plates. A sterile cotton swab was used to spread the bacterial inoculum evenly on a sterile Petri dish containing MH agar. The agar was then punched with four wells of 6 mm in diameter using a cork borer for different concentrations, including 30, 60, and 90 µL, and one for the control group (ZnO NPs Supernatant as control). Under aerobic conditions, the plates were then incubated for 24 h at 36 °C ± 1 °C. Confluent bacterial growth was observed after incubation. Bacterial growth inhibition was measured in millimeters.

The level of ZnO nanoparticle exposure on cultures was evaluated using time–kill kinetics assay. New cultures were grown in nanoparticles containing a medium as a test, while others were grown without the addition of the nanoparticles as a control [17,24].

3. Results and Discussion

3.1. UV–Visible Spectrophotometer Analysis

A change in the initial pale-white color was observed via UV analysis [25,26] after the 3rd h of the reaction, irrespective of the precursor concentration used, over the 24 h incubation period. UV spectra were recorded in absorption mode over a range of wavelengths from 300 to 800 nm. The control exhibited a distinctive absorption peak at 510 nm, which was confirmed via observation. As a result of the inclusion of hexagonal ZnO nanoparticles, this peak shifted within the 450–550 nm range at different treatment times. In the samples treated for 6 h, absorption peaks were discovered at 380 nm, as illustrated in Figure 1. The absorption wavelength was found to increase with the treatment time due to the increased amount of crystalline ZnO on the surface. Similar results were observed with cumin seeds [27], *Moringa oleifera* [28], *Nyctanthes* flower [19], *Eclipta alba* [29], and *Ulva lactuca* seaweed [30], with a maximum wavelength of 320–400 nm.

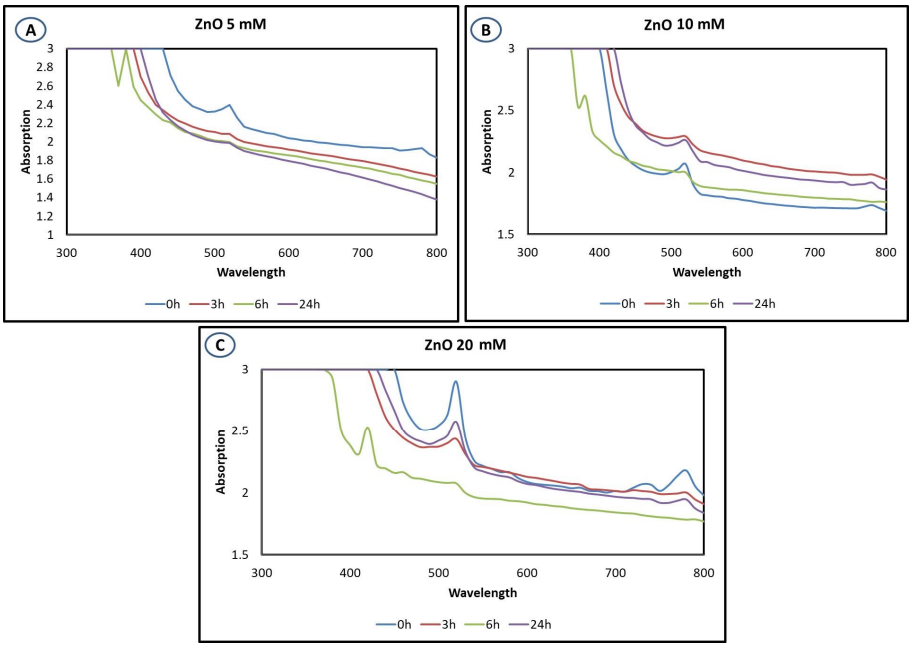

Figure 1. UV–Visible spectra of ZnO nanoparticles at (**A**) 5 mM, (**B**) 10 mM, and (**C**) 20 mM concentrations.

3.2. Powdered X-ray Diffraction Analysis

PXRD is an analytical technique that uses scattered X-rays to detect and identify nanoparticles based on their crystal structure and crystallite size. This effective, non-destructive tool is useful for analyzing powders, thin films, and single crystals as well a wide range of nanoparticles. It is a critical technique because crystal structure and crystallite size can impact the properties and potential applications of nanoparticles [31–33].

The X-ray diffraction peaks were obtained from the hexagonal phase of ZnO (JCPDS data card 89-0510). The purity and crystal structures of the probiotic-bacteria-mediated ZnO nanoparticles with various concentrations were obtained (Figure 2). These various concentrations yielded the same lattice planes of (100), (002), (101), and (002), which correspond to the 2θ values of 22.2°, 23.7°, 24.8°, and 31.3°, respectively. The crystal size, X-ray wavelength, Bragg's angle, and full width at half maximum of the (1 0 1) peak were used to calculate the nanoparticle size using Scherrer's formula ($D = 0.9\ \lambda/(\beta\ \mathrm{Cos}\ \theta)$). The calculated size was nearly 110 nm, which fell within the range of other ZnO nanoparticles synthesized using *Aloe barbadensis* leaf extract [34]; prepared via the hydrothermal growth method [35] or using *Ulva fasciata* [36]; and from the pods of *Parkia roxburghii* [37].

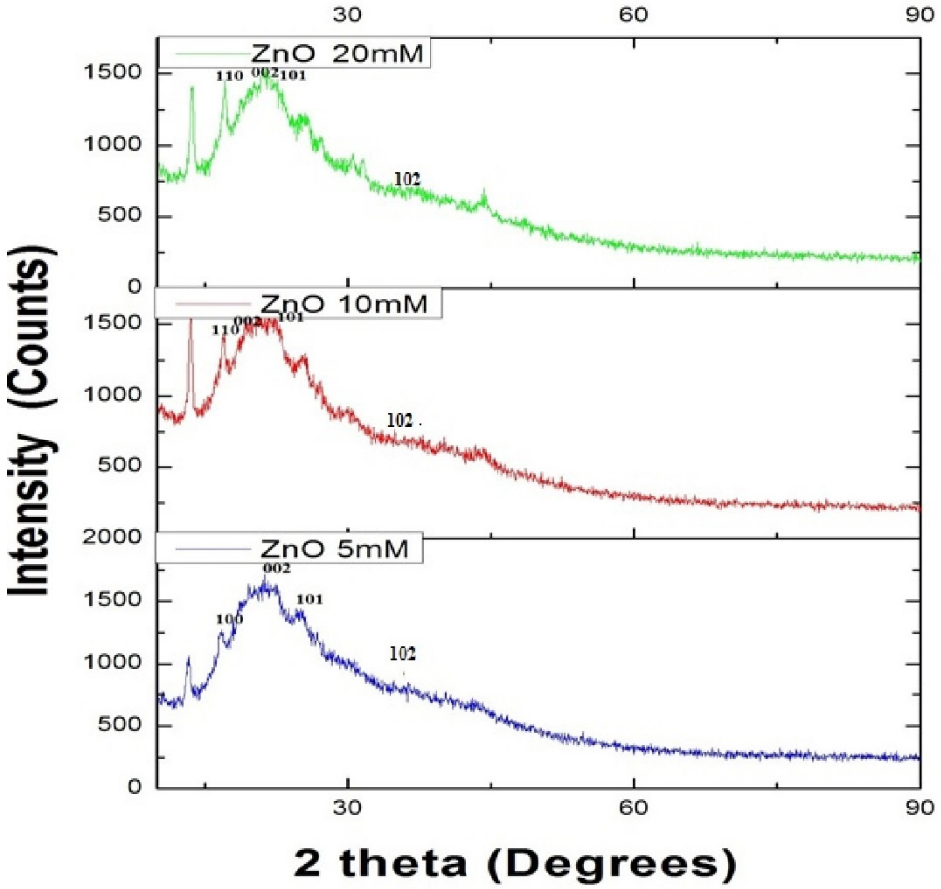

Figure 2. XRD analysis of ZnO NPs at different concentrations (5 mM, 10 mM, and 20 mM).

3.3. Identification of Compound Interaction

In the present research, FTIR was used to determine the functional groups on the surface of the synthetized ZnO NPs [38–40]. The FT-IR spectra of the 5 mM ZnO nanoparticles showed prominent peaks, as depicted in Figure 3. The presence of OH groups, which was due to phenolic, alcoholic, and acid groups, is indicated by the broad peak at 3282 cm^{-1}. The presence of H-C-H asymmetric and symmetric stretching, which occurred due to the presence of alkane groups, is indicated by the peak at 2931 cm^{-1}. The peak at 1726 cm^{-1} was attributed to the C=O group, whose presence was due to ketone, ester, and carboxylic acid functional groups. The peak at 1637 cm^{-1} is linked to the presence of C=O, whose presence was due to an amide group. Similarly, due to an amide group, the peak at 1531 cm^{-1} also suggests the presence of a C=O group.

The major peaks in the FT-IR spectra of the ZnO 10 mM nanoparticles evidenced the presence of OH groups, occurring due to the presence of phenolic, alcoholic, and acid groups, which was indicated by the peak at 3273 cm^{-1} (wide peak). The peaks at 2966 and 2931 cm^{-1} indicate H-C-H asymmetric and symmetric stretching.

The peaks at 1450 and 1379 cm^{-1} confirm the existence of N=O. The peaks in the FT-IR spectra of the ZnO 20 mM nanoparticles confirmed the presence of OH groups, which appeared due to the presence of phenolic, alcoholic, and ketone groups, as indicated by the broad peak at 3292 cm^{-1}. The peak at 2929 cm^{-1} indicates H-C-H asymmetric and symmetric stretching due to the presence of an alkane group. The peak of the C=O group, which appeared due to the presence of esters, ketones, and carboxylic acids, is indicated at 1726 cm^{-1}. The peak showed the presence of C=O due to an amide group at 1633.71. The presence of another C=O due to the existence of an amide group is indicated by the peak at 1531 cm^{-1}. The peak at 1381 cm^{-1} indicates the presence of an N=O group. The peaks at 1288, 1180, and 1053 cm^{-1} indicate the occurrence of a C-O group, which existed due to

the presence of esters and ethers. Therefore, regardless of the concentration, the functional groups are the same.

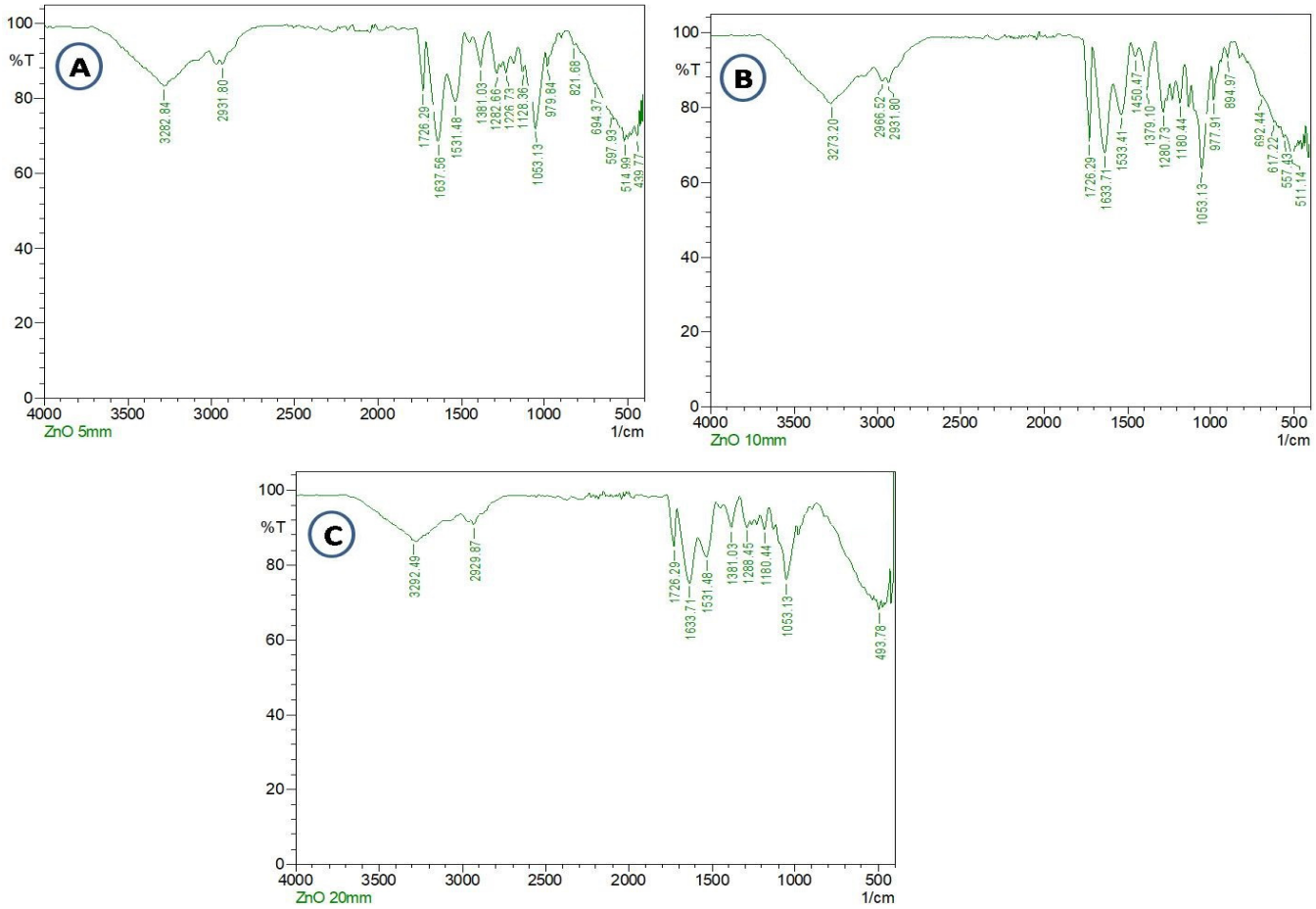

Figure 3. FTIR analysis of ZnO NPs at different concentrations. (**A**) 5 mM, (**B**) 10 mM, and (**C**) 20 mM concentrations.

3.4. SEM Analysis

SEM uses a focused beam of electrons to scan a sample and create high-resolution images of its surface by interacting with the atoms to emit secondary electrons, backscattered electrons, and X-rays. It is useful for analyzing a wide range of materials, including nanoparticles, and can provide detailed images of their shape, size, and distribution [41,42].

A scanning electron microscope was used to carry out research on the surface morphology of the ZnO nanoparticles. Measurements were taken to analyze the synthesized nanostructure's growth and morphological properties. The SEM results revealed the presence of the synthesized zinc oxide nanoparticles as micro-sized ZnO bioconjugates with a size range of 100–120 nm, as shown in Figure 4. When ZnO NPs are synthesized in an aqueous medium, the surface energy increases and the space between the particles narrows due to densification [43]. A similar morphology was observed with ZnO nanoparticles synthesized via the sol–gel method, in the flower twigs of *Elaeagnus angustifolia* [44], in *Tabernaemontana divaricata* leaf extract [21], and in *E. globulus* leaves [45].

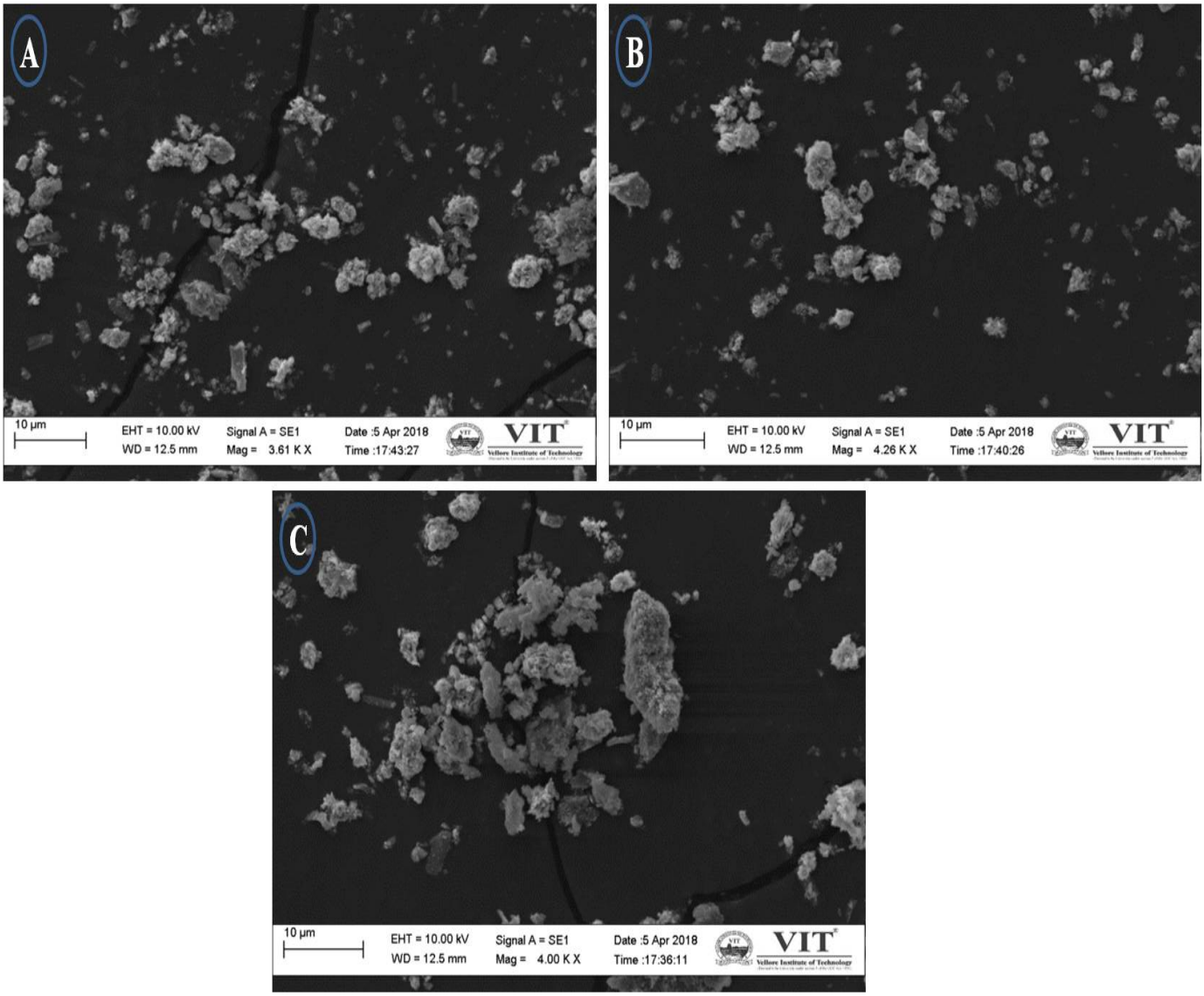

Figure 4. SEM analysis of ZnO nanoparticles at (**A**) 5 mM, (**B**) 10 mM, and (**C**) 20 mM concentrations.

3.5. AFM Analysis

AFM entails the scanning of the surface of a sample using a sharp tip and measuring the forces between the tip and the sample. This allows for the high-resolution imaging of samples at the nanoscale and the characterization of nanoparticles in terms of their size, shape, distribution, mechanical properties, and chemical composition. AFM has found wide applications in materials science, biology, and chemistry [46,47].

In Figure 5, it is evident that the ZnO nanoparticles are monodispersed with a clearly spherical morphology. The mean particle size is about 90–100 nm, and the degree of roughness is about 3 nm. The particles are tightly packed and evenly distributed. The results show that the diameter (D) of the ZnO particles in the monolayer is approximately 7.5–11.1 nm.

The monodispersity of particles is an important aspect that gives rise to their consistent size and shape, leading to efficient reactions in catalysis and improved pharmacokinetics in drug delivery. A spherical morphology is beneficial for drug delivery, while tight packing and even distribution can improve the performance of solar cells or sensors. The presence of small ZnO nanoparticles in monolayers may also improve the electronic properties of electronic devices [48–50]. In previous research, the AFM results of marine-yeast-mediated

ZnO nanoparticles demonstrated that the shape of the NPs was round and that their size was 86.27 nm [51].

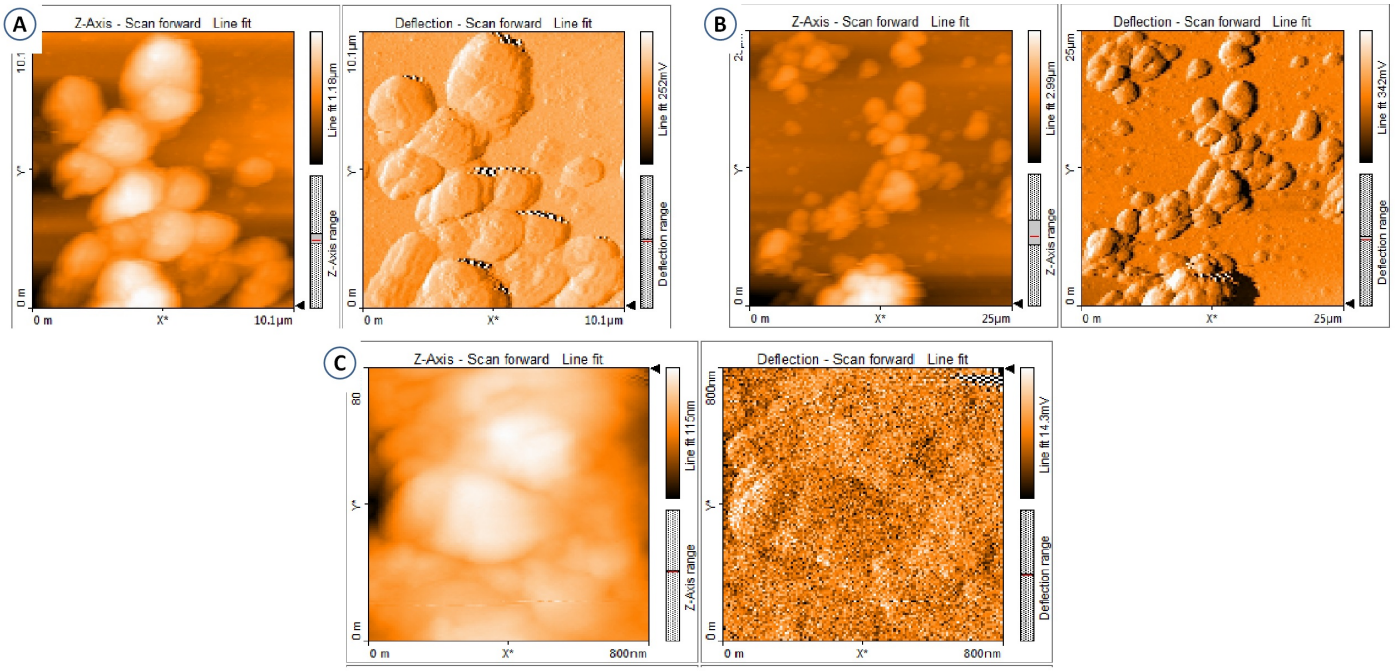

Figure 5. AFM images of ZnO NPs at (**A**) 5 mM, (**B**) 10 mM, and (**C**) 20 mM concentrations. * Axis.

3.6. Antibacterial Activity of Zinc Oxide Nanoparticles

The antibacterial activity of the ZnO nanoparticles was determined via their exposure to fish pathogens and gauging the extent of inhibited bacterial growth [52]. ZnO nanoparticles can manifest their antibacterial activity through various mechanisms. One of these mechanisms includes the dismemberment of the bacterial cell membrane, which eventually results in the death of the bacterial cell. The production of reactive oxygen species (ROS), such as hydrogen peroxide, is yet another process that contributes to the death of bacterial cells. ROS, such as hydrogen peroxide, may damage DNA and proteins, ultimately resulting in cell death. Furthermore, the nanoparticles can interact with the bacterial cell surface, thereby hindering bacterial metabolism and reproduction [53,54].

An antibacterial study of three different concentrations (5, 10, and 20 mM) of the ZnO NPs' (30, 60, and 90 µg/mL) activity against fish pathogens, including *Serratia marcescens*, *Aeromonas hydrophilla*, *Vibrio harveyi*, and *Vibrio parahaemolyticus*, was performed. According to Figure 6, the maximum activity was observed for *Vibrio harveyi*, which occurred at a 20 mM concentration. When the growth kinetics were evaluated for the ZnO nanoparticles at a 20 mM concentration for an incubation period of 24 h, it was further proven that the ZnO nanoparticles successfully inhibited the growth of the *Vibrio harveyi* culture as well as *Aeromonas hydrophila*, as demonstrated in Figures 7 and 8. The supernatant was used as negative control. In a prior study, durian-rind-synthesized ZnO NPs showed significant antibacterial efficacy against *Escherichia coli* and *Staphylococcus aureus*. Zinc ions released by ZnO NPs harm the bacterial cell membrane and undermine its integrity, thereby killing a bacterium [55]. The biosynthesis of nanoparticles through green approaches, as conducted in this research, has been receiving an increasing amount of attention due to its eco-friendliness, low cost, and biocompatibility [56].

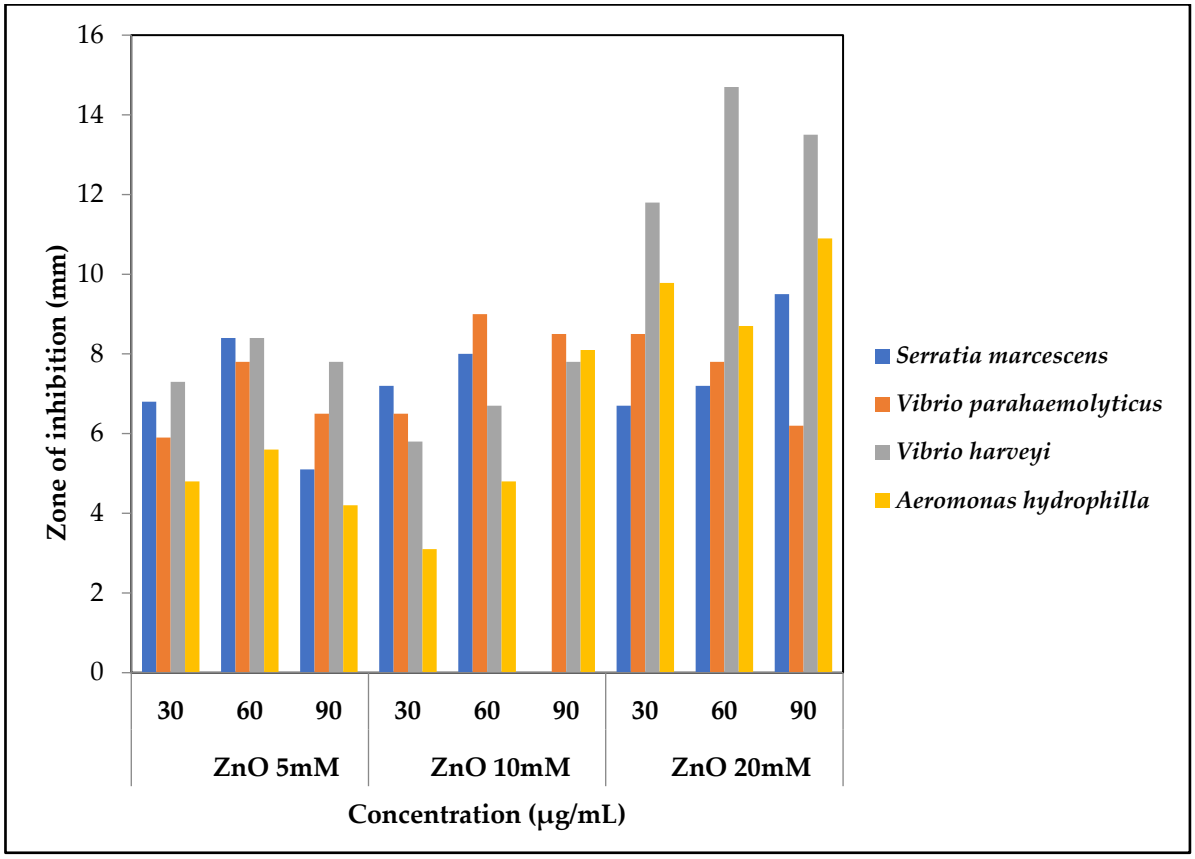

Figure 6. Antibacterial activity of ZnO nanoparticles determined via their zone of inhibition against various fish pathogens.

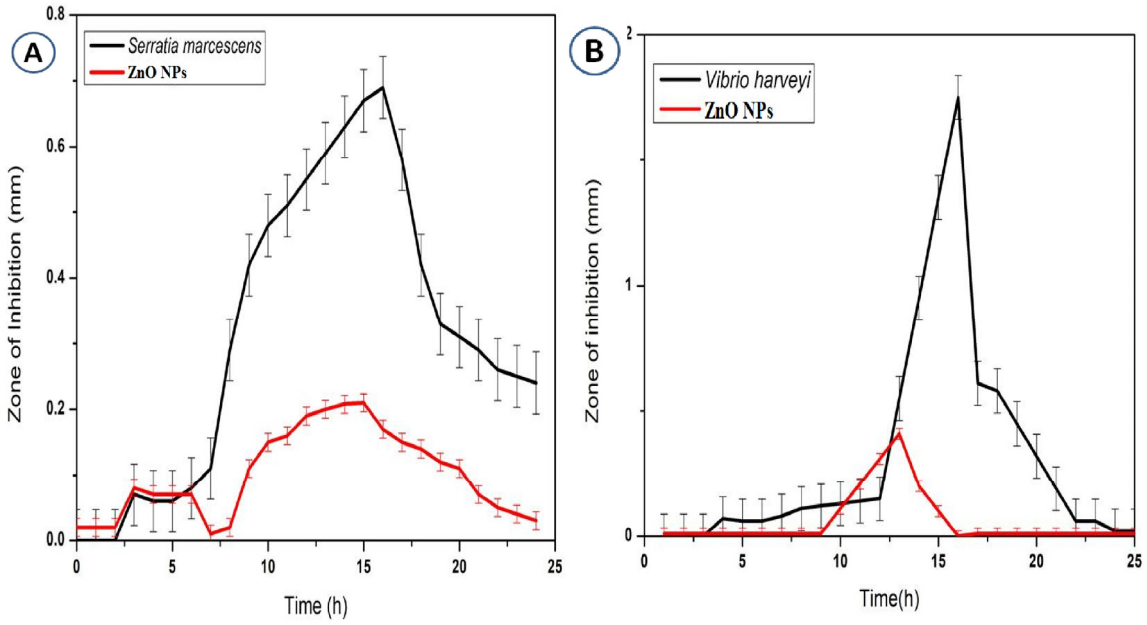

Figure 7. Time–kill kinetics of biosynthesized ZnO NPs against (**A**) *Serratia marcescens* and (**B**) *Vibrio harveyi*.

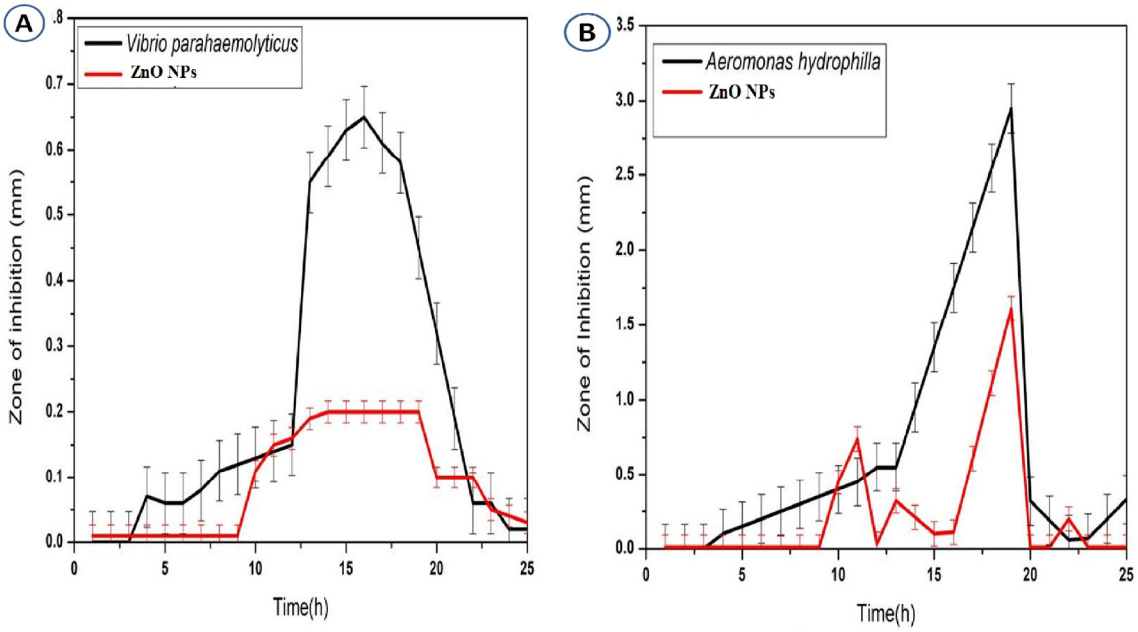

Figure 8. Time–kill kinetics of biosynthesized ZnO NPs against (**A**) *Vibrio parahaemolyticus* and (**B**) *Aeromonas hydrophilla*.

ZnO NPs may have many antibacterial mechanisms. ROS (reactive oxygen species) impair cell membrane integrity, oxidizing lipids, proteins, and DNA. Depending on their form and size, ZnO NPs may be ingested through endocytosis, nonspecific uptake, or membrane diffusion via membrane-based holes. Nanoparticles attach to cells via the electrostatic attraction of Zn^{+2} ions to negatively charged surfaces. Gram-negative bacteria are more sensitive to nanoparticle toxicity due to their weaker peptidoglycan coating. This is because thinner peptidoglycan layers provide a less efficient barrier for the interactions between the nanoparticles and the cell membrane. As nanoparticles come into direct contact with bacteria, factors such as the cell wall's thickness, structure, and composition influence their effects. The inhibition of enzymes by nanoparticles is an important component of the whole process of the induction of the death of bacterial cells. They also have the ability to suppress efflux pumps, which renders the cultures bactericidal [29,32,57,58].

4. Conclusions

The biogenic production of ZnO nanoparticles utilizing *L. fermentum* and the resulting NPs' characterization and effectiveness against fish pathogens were shown in this work. Regarding bactericidal action, a high concentration of ZnO NPs is very crucial. In this study, the nanoparticles were created using the probiotic bacterial culture *Lactobacillus fermentum*, for which no toxic chemicals or reagents were used in the synthetic process. SEM, XRD, FTIR, AFM, and UV–visible spectrophotometry were used to analyze the morphology and maximum absorbance of the biosynthesized ZnO NPs. The mechanism behind the developed NPs' actions may be attributed to their easy penetration into the cell membranes, ROS generation, efflux pump inhibition, and their morphology. The study's findings reveal that ZnO NPs exhibit potent antimicrobial properties against fish pathogens and that the effectiveness of this technique's antibacterial activity is directly proportional to the dose of the nanoparticles. These findings suggest that ZnO NPs have the potential to act as a natural alternative to traditional antibiotics for the control of fish pathogens, which is also significant in consideration of the massive use of antibiotics in aquaculture and the increasing resistance phenomenon. However, further study is required to evaluate ZnO NPs' safety and efficacy in fish farming. Aquaculture is an increasingly fundamental source of seafood, for which an increasing use of antibiotics has been reported [59]. The future of aquaculture is dependent on the outcome of addressing this challenge [60]. In addition,

inquiries might be broadened to examine the effect of ZnO NPs on other types of fish diseases and aquatic species in order to investigate their potential uses.

Author Contributions: Conceptualization, R.S. and S.J.; methodology, R.S.; software, R.S.; validation, R.S., S.J. and M.G.; formal analysis, R.S. and T.M.; investigation, R.S.; resources, K.A.A.-G.; data curation, M.G.; writing—original draft preparation, R.S.; writing—review and editing, M.G., M.N., N.S. and K.A.A.-G.; visualization, R.S.; supervision, R.S.; funding acquisition, K.A.A.-G. All authors have read and agreed to the published version of the manuscript.

Funding: This research was funded by King Saud University, grant number RSP2023R48.

Institutional Review Board Statement: Not applicable.

Informed Consent Statement: Not applicable.

Data Availability Statement: Not applicable.

Acknowledgments: The authors express their sincere appreciation to the Researchers Supporting Project Number (RSP2023R48), King Saud University, Riyadh, Saudi Arabia. The authors would like to thank the Vellore Institute of Technology, Tamil Nadu, India, for their encouragement and support. The authors thank the Peoples Friendship University of Russia, (RUDN University), Russia.

Conflicts of Interest: The authors declare no conflict of interest.

References

1. Emmett, R.; Akkersdyk, S.; Yeatman, H.; Meyer, B.J. Expanding awareness of docosahexaenoic acid during pregnancy. *Nutrients* **2013**, *5*, 1098–1109. [CrossRef] [PubMed]
2. Cillero, I.H.; Gil, J.; Irazusta, A.; Torres-Unda, J.; Zarrazquin, I.; Ruiz, F.; Irazusta, J.; Kortajarena, M. Longitudinal study: Lifestyle and cardiovascular health in health science students. *Nutr. Hosp.* **2014**, *30*, 1144–1151.
3. Centers for Disease Control and Prevention. *Get Smart: Know When Antibiotics Work*; Centers for Disease Control: Atlanta, GA, USA, 2010. Available online: www.cdc.gov/Features/GetSmart (accessed on 23 March 2023).
4. Marshall, B.M.; Levy, S.B. Food animals and antimicrobials: Impacts on human health. *Clin. Microbiol. Rev.* **2011**, *24*, 718–733. [CrossRef]
5. Heinitz, M.L.; Ruble, R.D.; Wagner, D.E.; Tatini, S.R. Incidence of *Salmonella* in fish and seafood. *J. Food Prot.* **2000**, *63*, 579–592. [CrossRef] [PubMed]
6. Lenchenko, E.; Lenchenko, S.; Sachivkina, N.; Kuznetsova, O.; Ibragimova, A. Interaction of *Cyprinus carpio* Linnaeus with the biofilm-forming *Aeromonas hydrophila*. *Vet. World* **2022**, *15*, 2458–2465. [CrossRef] [PubMed]
7. Babitha, S.; Korrapati, P.S. Biosynthesis of titanium dioxide nanoparticles using a probiotic from coal fly ash effluent. *Mater. Res. Bull.* **2013**, *48*, 4738–4742. [CrossRef]
8. Bahrulolum, H.; Nooraei, S.; Javanshir, N.; Tarrahimofrad, H.; Mirbagheri, V.S.; Easton, A.J.; Ahmadian, G. Green synthesis of metal nanoparticles using microorganisms and their application in the agrifood sector. *J. Nanobiotechnol.* **2021**, *19*, 86. [CrossRef]
9. Bandeira, M.; Giovanela, M.; Roesch-Ely, M.; Devine, D.M.; da Silva Crespo, J. Green synthesis of zinc oxide nanoparticles: A review of the synthesis methodology and mechanism of formation. *Sustain. Chem. Pharm.* **2020**, *15*, 100223. [CrossRef]
10. Hill, C.; Guarner, F.; Reid, G.; Gibson, G.R.; Merenstein, D.J.; Pot, B.; Morelli, L.; Canani, R.B.; Flint, H.J.; Salminen, S.; et al. Expert consensus document: The International Scientific Association for Probiotics and Prebiotics consensus statement on the scope and appropriate use of the term probiotic. *Nat. Rev. Gastroenterol. Hepatol.* **2014**, *11*, 504–516. [CrossRef]
11. Król, A.; Railean-Plugaru, V.; Pomastowski, P.; Złoch, M.; Buszewski, B. Mechanism study of intracellular zinc oxide nanocomposites formation. *Colloids Surf. A Physicochem. Eng. Asp.* **2018**, *553*, 349–358. [CrossRef]
12. Mohd Yusof, H.; Mohamad, R.; Zaidan, U.H.; Rahman, A. Microbial synthesis of zinc oxide nanoparticles and their potential application as an antimicrobial agent and a feed supplement in animal industry: A review. *J. Anim. Sci. Biotechnol.* **2019**, *10*, 57. [CrossRef] [PubMed]
13. Vallee, B.L.; Falchuk, K.H. The biochemical basis of zinc physiology. *Physiol. Rev.* **1993**, *73*, 79–118. [CrossRef]
14. Raja, A.; Ashokkumar, S.; Pavithra Marthandam, R.; Jayachandiran, J.; Khatiwada, C.; Kaviyarasu, K.; Ganapathi Raman, R.; Swaminathan, M. Eco-friendly preparation of zinc oxide nanoparticles using *Tabernaemontana divaricata* and its photocatalytic and antimicrobial activity. *J. Photochem. Photobiol. B Biol.* **2018**, *181*, 53–58. [CrossRef]
15. Rajiv, P.; Vanathi, P. Effect of Parthenium based vermicompost and zinc oxide nanoparticles on growth and yield of *Arachis hypogaea* L. in the zinc-deficient soil. *Biocatal. Agric. Biotechnol.* **2018**, *13*, 251–257. [CrossRef]
16. Dumbrava, A.; Berger, D.; Matei, C.; Radu, M.D.; Gheorghe, E. Characterisation and applications of a new composite material obtained by green synthesis, through deposition of zinc oxide onto calcium carbonate precipitated in green seaweeds extract. *Ceram. Int.* **2018**, *44*, 4931–4936. [CrossRef]

17. Patil, B.N.; Taranath, T.C. *Limonia acidissima* L. leaf mediated synthesis of silver and zinc oxide nanoparticles and their antibacterial activities. *Microb. Pathog.* **2018**, *115*, 227–232. [CrossRef] [PubMed]
18. Santhoshkumar, J.; Kumar, S.V.; Rajeshkumar, S. Synthesis of zinc oxide nanoparticles using plant leaf extract against urinary tract infection pathogen. *Resour.-Effic. Technol.* **2017**, *3*, 459–465. [CrossRef]
19. Jamdagni, P.; Khatri, P.; Rana, J.S. Green synthesis of zinc oxide nanoparticles using flower extract of *Nyctanthes arbor-tristis* and their antifungal activity. *J. King Saud Univ. Sci.* **2018**, *30*, 168–175. [CrossRef]
20. Ghayempour, S.; Montazer, M. Ultrasound irradiation based in-situ synthesis of star-like Tragacanth gum/zinc oxide nanoparticles on cotton fabric. *Ultrason. Sonochem.* **2017**, *34*, 458–465. [CrossRef]
21. Elumalai, K.; Velmurugan, S. Green synthesis, characterisation and antimicrobial activities of zinc oxide nanoparticles from the leaf extract of *Azadirachta indica* (L.). *Appl. Surf. Sci.* **2015**, *345*, 329–336. [CrossRef]
22. Amith Yadav, H.; Eraiah, B.; Nagabhushana, H.; Daruka Prasad, B.; Basavaraj, R.B.; Sateesh, M.K.; Shabaaz Begum, J.P.; Darshan, G.P.; Vijayakumar, G.R. Broad spectral inhibitory effects of pale green zinc oxide nanophosphor on bacterial and fungal pathogens. *Arab. J. Chem.* **2018**, *11*, 324–342. [CrossRef]
23. Menon, S.; Devi Ks, S.; Santhiya, R.; Rajeshkumar, S.; Venkat Kumar, S. Selenium nanoparticles: A potent chemotherapeutic agent and an elucidation of its mechanism. *Colloids Surf. B* **2018**, *170*, 280–292. [CrossRef]
24. Khatami, M.; Alijani, H.Q.; Heli, H.; Sharifi, I. Rectangular shaped zinc oxide nanoparticles: Green synthesis by *Stevia* and its biomedical efficiency. *Ceram. Int.* **2018**, *44*, 15596–15602. [CrossRef]
25. Passos, M.L.; Saraiva, M.L. Detection in UV-visible spectrophotometry: Detectors, detection systems, and detection strategies. *Measurement* **2019**, *135*, 896–904. [CrossRef]
26. Adeeyinwo, C.E.; Okorie, N.N.; Idowu, G.O. Basic calibration of UV/visible spectrophotometer. *Int. J. Sci. Technol.* **2013**, *2*, 247–251.
27. Zare, E.; Pourseyedi, S.; Khatami, M.; Darezereshki, E. Simple biosynthesis of zinc oxide nanoparticles using nature's source, and it's in vitro bio-activity. *J. Mol. Struct.* **2017**, *1146*, 96–103. [CrossRef]
28. Archana, B.; Manjunath, K.; Nagaraju, G.; Chandra Sekhar, K.B.; Kottam, N. Enhanced photocatalytic hydrogen generation and photostability of ZnO nanoparticles obtained via green synthesis. *Int. J. Hydrogen Energy* **2018**, *42*, 5125–5131. [CrossRef]
29. Singh, A.K.; Pal, P.; Gupta, V.; Yadav, T.P.; Gupta, V.; Singh, S.P. Green synthesis, characterisation and antimicrobial activity of zinc oxide quantum dots using *Eclipta alba*. *Mater. Chem. Phys.* **2018**, *203*, 40–48. [CrossRef]
30. Ishwarya, R.; Vaseeharan, B.; Kalyani, S.; Banumathi, B.; Govindarajan, M.; Alharbi, N.S.; Kadaikunnan, S.; Al-anbr, M.N.; Khaled, J.M.; Benelli, G. Facile green synthesis of zinc oxide nanoparticles using Ulva lactuca seaweed extract and evaluation of their photocatalytic, anti-biofilm and insecticidal activity. *J. Photochem. Photobiol. B Biol.* **2018**, *178*, 249–258. [CrossRef] [PubMed]
31. Bunaciu, A.A.; UdriŞTioiu, E.G.; Aboul-Enein, H.Y. X-ray diffraction: Instrumentation and applications. *Crit. Rev. Anal. Chem.* **2015**, *45*, 289–299. [CrossRef]
32. Padrela, L.; de Azevedo, E.G.; Velaga, S.P. Powder X-ray diffraction method for the quantification of cocrystals in the crystallization mixture. *Drug Dev. Ind. Pharm.* **2012**, *38*, 923–929. [CrossRef] [PubMed]
33. Thakral, N.K.; Zanon, R.L.; Kelly, R.C.; Thakral, S. Applications of powder X-ray diffraction in small molecule pharmaceuticals: Achievements and aspirations. *J. Pharm. Sci.* **2018**, *107*, 2969–2982. [CrossRef] [PubMed]
34. Sangeetha, G.; Rajeshwari, S.; Venckatesh, R. Green synthesis of zinc oxide nanoparticles by *Aloe barbadensis miller* leaf extract: Structure and optical properties. *Mater. Res. Bull.* **2011**, *46*, 2560–2566. [CrossRef]
35. Micova, J.; Buryi, M.; Simek, D.; Drahokoupil, J.; Neykova, N.; Chang, Y.Y.; Remes, Z.; Pop-Georgievski, O.; Svoboda, J.; Im, C. Synthesis of zinc oxide nanostructures and comparison of their crystal quality. *Appl. Surf. Sci.* **2018**, *461*, 190–195. [CrossRef]
36. Bhutiya, P.L.; Mahajan, M.S.; Abdul Rasheed, M.; Pandey, M.; Zaheer Hasan, S.; Misra, N. Zinc oxide nanorod clusters deposited seaweed cellulose sheet for antimicrobial activity. *Int. J. Biol. Macromol.* **2018**, *112*, 1264–1271. [CrossRef]
37. Paul, B.; Vadivel, S.; Dhar, S.S.; Debbarma, S.; Kumaravel, M. One-pot green synthesis of zinc oxide nano rice and its application as sonocatalyst for degradation of organic dye and synthesis of 2-benzimidazole derivatives. *J. Phys. Chem. Solids* **2017**, *104*, 152–159. [CrossRef]
38. Zarnowiec, P.; Lechowicz, L.; Czerwonka, G.; Kaca, W. Fourier transform infrared spectroscopy (FTIR) as a tool for the identification and differentiation of pathogenic bacteria. *Curr. Med. Chem.* **2015**, *22*, 1710–1718. [CrossRef]
39. Mohammed, A.; Abdullah, A. Scanning electron microscopy (SEM): A review. In Proceedings of the 2018 International Conference on Hydraulics and Pneumatics—HERVEX, Băile Govora, Romania, 7–9 November 2018; Volume 7, pp. 7–9.
40. Lemine, O.M. Microstructural characterisation of α-Fe_2O_3 nanoparticles using, XRD line profiles analysis, FE-SEM and FT-IR. *Superlattices Microstruct.* **2009**, *45*, 576–582. [CrossRef]
41. Simonet, B.M.; Valcárcel, M. Monitoring nanoparticles in the environment. *Anal. Bioanal. Chem.* **2009**, *393*, 17–21. [CrossRef]
42. Janaki, A.C.; Sailatha, E.; Gunasekaran, S. Synthesis, characteristics and antimicrobial activity of ZnO nanoparticles. *Spectrochim. Acta Part A Mol. Biomol. Spectrosc.* **2015**, *144*, 17–22. [CrossRef]
43. Akbari, A.; Khammar, M.; Taherzadeh, D.; Rajabian, A.; Khorsand Zak, A.; Darroudi, M. Zinc-doped cerium oxide nanoparticles: Sol-gel synthesis, characterisation, and investigation of their in vitro cytotoxicity effects. *J. Mol. Struct.* **2017**, *1149*, 771–776. [CrossRef]
44. Singh, A.; Singh, N.B.; Hussain, I.; Singh, H.; Yadav, V.; Singh, S.C. Green synthesis of nano zinc oxide and evaluation of its impact on germination and metabolic activity of *Solanum lycopersicum*. *J. Biotechnol.* **2016**, *233*, 84–94. [CrossRef]

45. Siripireddy, B.; Mandal, B.K. Facile green synthesis of zinc oxide nanoparticles by *Eucalyptus globulus* and their photocatalytic and antioxidant activity. *Adv. Powder Technol.* **2017**, *28*, 785–797. [CrossRef]
46. Agarwal, H.; Menon, S.; Venkat Kumar, S.; Rajeshkumar, S. Mechanistic study on antibacterial action of zinc oxide nanoparticles synthesised using green route. *Chem. Biol. Interact.* **2018**, *286*, 60–70. [CrossRef] [PubMed]
47. Hoo, C.M.; Starostin, N.; West, P.; Mecartney, M.L. A comparison of atomic force microscopy (AFM) and dynamic light scattering (DLS) methods to characterize nanoparticle size distributions. *J. Nanopart. Res.* **2008**, *10*, 89–96. [CrossRef]
48. Sajja, S.; Chandler, M.; Fedorov, D.; Kasprzak, W.K.; Lushnikov, A.; Viard, M.; Shah, A.; Dang, D.; Dahl, J.; Worku, B.; et al. Dynamic behavior of RNA nanoparticles analyzed by AFM on a mica/air interface. *Langmuir* **2018**, *34*, 15099–15108. [CrossRef]
49. Omidi, E.; Korayem, A.H.; Korayem, M.H. Sensitivity analysis of nanoparticles pushing manipulation by AFM in a robust controlled process. *Precis. Eng.* **2013**, *37*, 658–670. [CrossRef]
50. Baer, D.R.; Gaspar, D.J.; Nachimuthu, P.; Techane, S.D.; Castner, D.G. Application of surface chemical analysis tools for characterization of nanoparticles. *Anal. Bioanal. Chem.* **2010**, *396*, 983–1002. [CrossRef]
51. Aswathy, R.; Gabylis, B.; Anwesha, S.; Bhaskara Rao, K. Green synthesis and characterization of marine yeast-mediated silver and zinc oxide nanoparticles and assessment of their antioxidant activity. *Asian J. Pharm. Clin. Res.* **2017**, *10*, 235–240.
52. Slavin, Y.N.; Asnis, J.; Hńfeli, U.O.; Bach, H. Metal nanoparticles: Understanding the mechanisms behind antibacterial activity. *J. Nanobiotechnol.* **2017**, *15*, 65. [CrossRef]
53. Sirelkhatim, A.; Mahmud, S.; Seeni, A.; Kaus, N.H.; Ann, L.C.; Bakhori, S.K.; Hasan, H.; Mohamad, D. Review on zinc oxide nanoparticles: Antibacterial activity and toxicity mechanism. *Nano-Micro Lett.* **2015**, *7*, 219–242. [CrossRef] [PubMed]
54. Ravichandran, V.; Sumitha, S.; Ning, C.Y.; Xian, O.Y.; Kiew Yu, U.; Paliwal, N.; Shah, S.A.; Tripathy, M. Durian waste mediated green synthesis of zinc oxide nanoparticles and evaluation of their antibacterial, antioxidant, cytotoxicity and photocatalytic activity. *Green Chem. Lett. Rev.* **2020**, *13*, 102–116. [CrossRef]
55. Abdo, A.M.; Fouda, A.; Eid, A.M.; Fahmy, N.M.; Elsayed, A.M.; Khalil, A.M.; Alzahrani, O.M.; Ahmed, A.F.; Soliman, A.M. Green synthesis of Zinc Oxide Nanoparticles (ZnO-NPs) by *Pseudomonas aeruginosa* and their activity against pathogenic microbes and common house mosquito, *Culex pipiens*. *Materials* **2021**, *14*, 6983. [CrossRef]
56. Salem, W.; Leitner, D.R.; Zingl, F.G.; Schratter, G.; Prassl, R.; Goessler, W.; Reidl, J.; Schild, S. Antibacterial activity of silver and zinc nanoparticles against *Vibrio cholerae* and enterotoxic *Escherichia coli*. *Int. J. Med. Microbiol.* **2015**, *305*, 85–95. [CrossRef]
57. Gupta, A.; Srivastava, R. Zinc oxide nanoleaves: A scalable disperser-assisted sonochemical approach for synthesis and an antibacterial application. *Ultrason. Sonochem.* **2018**, *41*, 47–58. [CrossRef]
58. Saravanan, M.; Gopinath, V.; Chaurasia, M.; Syed, A.; Ameen, F.; Purushothaman, N. Green synthesis of anisotropic zinc oxide nanoparticles with antibacterial and cytofriendly properties. *Microb. Pathog.* **2018**, *115*, 57–63. [CrossRef] [PubMed]
59. Schar, D.; Klein, E.Y.; Laxminarayan, R.; Gilbert, M.; Van Boeckel, T.P. Global trends in antimicrobial use in aquaculture. *Sci. Rep.* **2020**, *10*, 21878. [CrossRef]
60. Chen, J.; Sun, R.; Pan, C.; Sun, Y.; Mai, B.; Li, Q.L. Antibiotics and Food Safety in Aquaculture. *J. Agric. Food Chem.* **2020**, *68*, 11908–11919. [CrossRef]